International Journal of Nanoelectronics and Materials
IJNeaM
ISSN 1985-5761 | E-ISSN 2232-1535

Impact of Laser Fluence on the Formation of T-Nb2O5 Nanostructure: A Study in a Liquid Environment

Evan T. Salim[a,*], Tamara E Abdulrahman[a], Raed Khalid Ibrahim[b], Zaid T. Salim[c], Rana O. Mahdi[a], Ahmed A. Al-Amiery[d], Subash C. B. Gopinath[e, f, g]

[a]*College of Applied Science, University of Technology-Iraq, Baghdad –Iraq*
[b]*Al-Farahidi University, Baghdad, Iraq*
[c]*College of Energy and Environmental Sciences, Al-Karkh University of Science, Baghdad 10081, Iraq*
[d]*Al-Ayen Scientific Research Center, Al-Ayen Iraqi University, AUIQ, P.O. Box: 64004, An Nasiriyah, Thi Qar, Iraq*
[e]*Center for Global Health Research, Saveetha Medical College & Hospital, Saveetha Institute of Medical and Technical Sciences (SIMATS), Thandalam, Chennai – 602 105, Tamil Nadu, India*
[f]*Faculty of Chemical Engineering & Technology & Institute of Nano Electronic Engineering, Universiti Malaysia Perlis (UniMAP), 02600 Arau, Perlis Malaysia*
[g]*Department of Technical Sciences, Western Caspian University, Baku AZ 1075, Azerbaijan*
**Correspondence author. E-mail: evan_tarq@yahoo.com, evan.t.salim@uotechnology.edu.iq; Tel.: + (964) 7715752087*

ABSTRACT

In this work, different laser fluencies ranges (8.1–17.8 J/cm2) and Nd: YAG of 1064 nm wavelength were studied and analyzed. Energy band gaps acquired ranged from 4.2 eV to 3.9 eV. X-ray diffraction (XRD) results revealed the formation of an orthorhombic (T-Nb2O5) niobium pentoxide nanostructure. The grain size of the Nb2O5 nanoparticles ranged from approximately 58.2 nm to 244.6 nm. TEM images showed spherical particles whose density increased with increasing laser fluence. Raman and Fourier-transform infrared (FTIR) spectra exhibited peaks indicating the formation of T phase-Nb2O5 nanomaterial.

Keywords: *Liquid-pulse laser ablation, Optical properties, Raman spectra, FTIR*

1. INTRODUCTION

Niobium pentoxide (Nb_2O_5) or niobium [1, 2] is a substantial n-type transition metal oxide semiconductor with unique properties. Thus, it has been applied to electrochromic devices, and sensors and develops highly efficient solar cells, [3-5]. This material has drawn great attention as a combination of different compounds, such as lithium niobite and barium, used in optical modulators and waveguides [6-8]. It is the most thermodynamically stable metal oxide featuring chemical inertness and a low cytotoxicity [9, 10]. The charge state of Nb_2O_5 is (5+) and has a lower electrical conductivity compared to other niobium oxides [11]. Besides, Nb_2O_5 absorbs Ultra Violet light with a 385nm wavelength or less and visible light to achieve high photo-catalytic efficiency[12, 13].

Niobia can either happen in an amorphous state or one of various crystalline polymorphs. In general, Nb_2O_5 can come in a powder-like structure of white color or a single crystal transparent form. The physical properties of the Nb_2O_5 can be ultimately changed according to its polymorph and the composition parameters and synthesizing method [14-16].

Nb_2O_5 has been prepared using various methods, such as metal oxidation in air, hydrolyzation of alkali niobates, niobium alkoxides [17], chemical reaction of hydrofluoric acid and ammonia, pulsed laser deposition[18, 19], reactive radio frequency magnetron sputtering [20], atomic layer deposition [21, 22], sol-gel [23], and other methods.

Joya et al. (2017)[24] fabricated an Nb_2O_5 orthorhombic structure by employing the sol-gel method, and SEM revealed unique structures (skeleton Nb_2O_5). Later, Wang et al. [25] prepared Nb_2O_5 nanowires using plasma-enhanced chemical vapor deposition. XRD data showed an orthorhombic T- Nb_2O_5 structure, Dai et al(2020)[26] prepared Nb_2O_5 nanofibers used the template, XRD revealed an orthorhombic Nb_2O_5 with different range band gaps. A monoclinic Nb_2O_5 was prepared by Fakhri et al. (2021)[27] they employed different conditions using a pulsed laser deposition system.

Material properties can be varied by tuning preparation conditions. The effect of laser energy on the properties of Nb_2O_5 in liquid is not extensively studied yet. This work aims to characterize the unique properties of Nb_2O_5 nanoparticles obtained by laser ablation in liquid by using a metal plate target.

2. MATERIAL AND METHOD

Nb_2O_5 nanoparticles were prepared under certain conditions and parameters. A high purity (about 99.999) Niobium plate manufactured by Sigma Aldrich was used with de-ionized water and Nd: YAG laser to achieve

nanoparticle preparation. Sample preparation process was maintained by submerging the niobium target into the de-ionized water and ablated by laser of parameters: 1 Hz, 150 pulse, and fluence ranges from 8.1 J/cm^2 to 17.8 J/cm^2. A Shimadzu 1800 spectrophotometer double-beam UV-VIS device was utilized to study the Nb_2O_5 optical properties.

FTIR spectroscopy was studied using BRUKER-7613 to achieve the chemical bonds of prepared materials. A SUNSHINE-V2-86 device was used to obtain the Raman spectrum. An X-ray diffraction system from (Shimadzu) with 0.15406 nm wavelength was employed to determine the structural characteristics of Nb_2O_5. The sample was scanned from 2θ of 15° to 50°. Niobia morphology, such as size, distribution, and particle shape, was investigated using a Titan 80-300 HRTEM device. For chemical composition, the stoichiometry and element percentages in the sample were investigated using inspect S50 (FEI Company/Netherland).

3. RESULTS AND DISCUSSION:

The X-ray diffraction pattern of the Nb_2O_5 samples is shown in Figure (1). The X-ray diffraction revealed several peaks cantered at different angles (2θ): 16.8°, 22.8°, 35.8°, 42.8°, 47.4°, and 48.4° which they are correspond to the planes (1 3 0), (0 0 1), (1 0 1), (1 13 0), (0 0 2) and (1 1 0). It was shown that the peaks belong to the orthorhombic structure of the T-Nb_2O_5 as consistence with the (00-030-0873) card. The diffraction peaks at 2θ =30.6° belong to the pure Nb as tabulated in (00-003-0905) JCPDS card and shown in other results [28-31].

The crystallite structure of the prepared Nb_2O_5 showed a significant enhancement in terms of laser fluency to reach 12.09 J/cm^2 with an evident reduction in the niobium diffraction peak of that fluency. As laser fluency increased to 17.82 J/cm^2, the diffraction peaks of the prepared sample became higher and more obvious with prominent development in the pure metal formation. Scherrer's formula was utilized to estimate the size of the particle of the prepared samples [32-34]

$$D = {k\lambda}/{(\beta \cos \theta)} \quad (1)$$

Where D is the particle size in nanometers, K is the shape factor, λ is 0.15406 nm (X-ray wavelength), β is spectrum broadening at the Full-Width Half-Maximum (FWHM), θ is Bragg angle, and finally, δ is dislocation density which can be calculated using the equation 2 [35-37]:

$$\delta = 1 \,/\, D_{XRD}^2 \quad (2)$$

It is worth mentioning that the shape (K) factor is about 0.9 and this value changes concerning the crystallite shape. The Micro-strains were obtained using the following formula [38-40]:

$$\eta = {\beta}/{4\tan\theta} \quad (3)$$

Table (1) presents the grain size of the Nb_2O_5 nanoparticles at different laser fluences. It can be recognized that the grain size is directly related to laser fluence due to the increase in the amount of the ablated material. This phenomenon led to particle agglomeration, which agrees with the TEM and UV-Vis results.

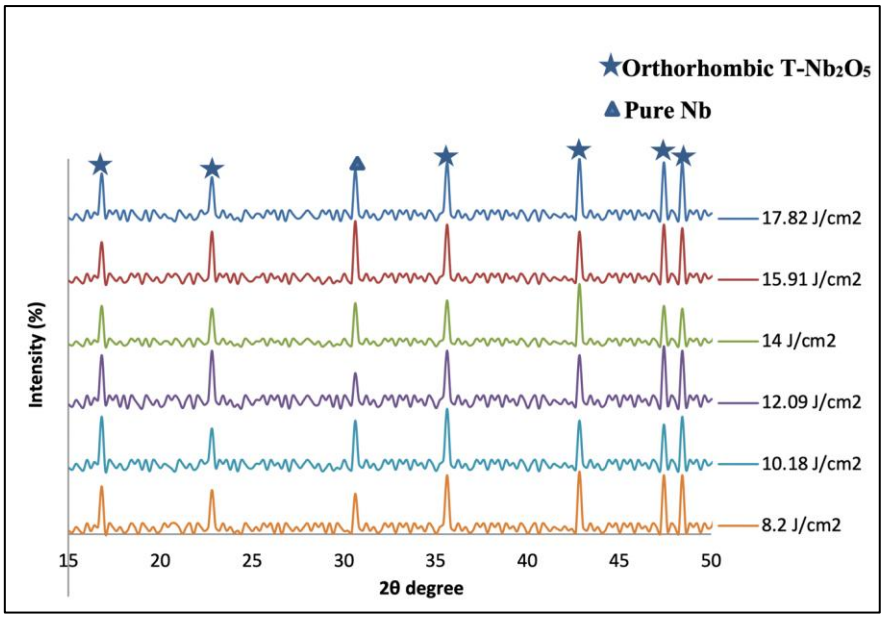

Figure 1. X-ray diffraction patterns of Nb_2O_5 samples using 150 pulses at different ranges of Nd-Yag laser fluencies.

Table 1 Grain size for different laser fluencies

2θ.	FWHM.	Miller indices	Grain size(nm)	Dislocation density(δ)	Microstrains
16.8°	0.141	1 3 0	58.245	0.294	5.2
22.8°	0.131	0 0 1	62.121	0.259	6.6
35.8°	0.069	1 0 1	114.559	0.076	5.5
42.8°	0.054	1 13 0	143.144	0.048	5.2
47.4°	0.045	0 0 2	169.194	0.034	4.8
48.4°	0.031	0 0 1	244.664	0.016	3.4

The energy bandgap and the absorption spectrum are presented in Figure (2). They are graphed as a function of the wavelength of Nb_2O_5 Nanomaterials. A clear red shift in the absorbance spectrum with laser fluence could be recognized. The obtained results indicate that the concentration of the ablated material is ultimately developed. Besides, the energy gap and laser fluence values were found to be inversely related.

This can be back to the fact that the size of the prepared nanoparticles is large enough compared to the exciton Bohr radius which results in a reduction in energy bandgap value due to the weakness confinement as shown in Table (2) [41-44]. These results strongly agree with the grain size obtained using XRD.

The estimation of the energy bandgap was conducted using Tauc's plot. It indicates that the incident photon energy to be on the horizontal axes (abscissa) and $(\alpha hv)^2$ is inordinate. The value of the energy bandgap was determined by the absorption edge for the direct interbond transition and the obtained from equation 4 given below [45-47]:

$$\alpha hv = c(hv - E_g)^{1/2} \quad (4)$$

Equation (4) parameters are defined as: α is the absorption coefficient, h is Plank's constant, v is the incident photon frequency, and finally c is the direct transition constant.

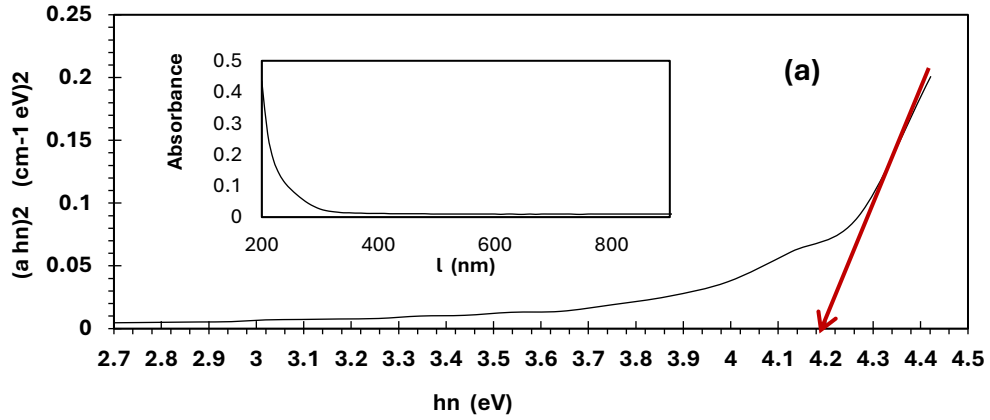

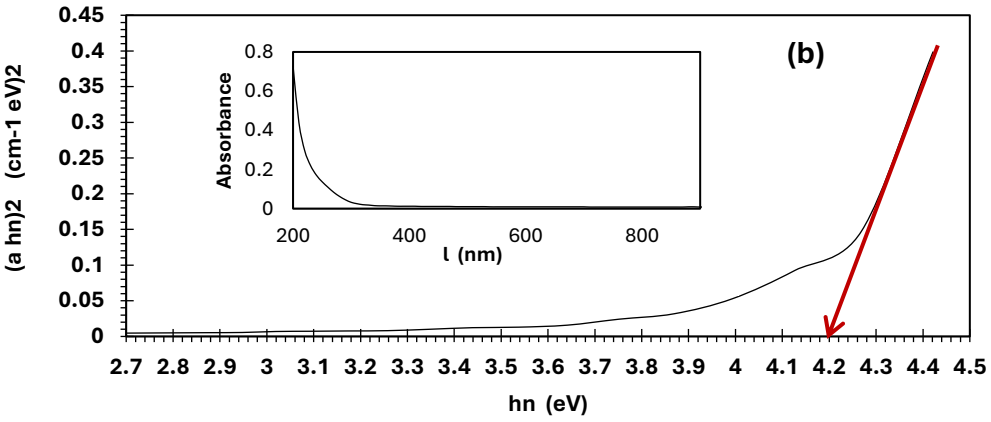

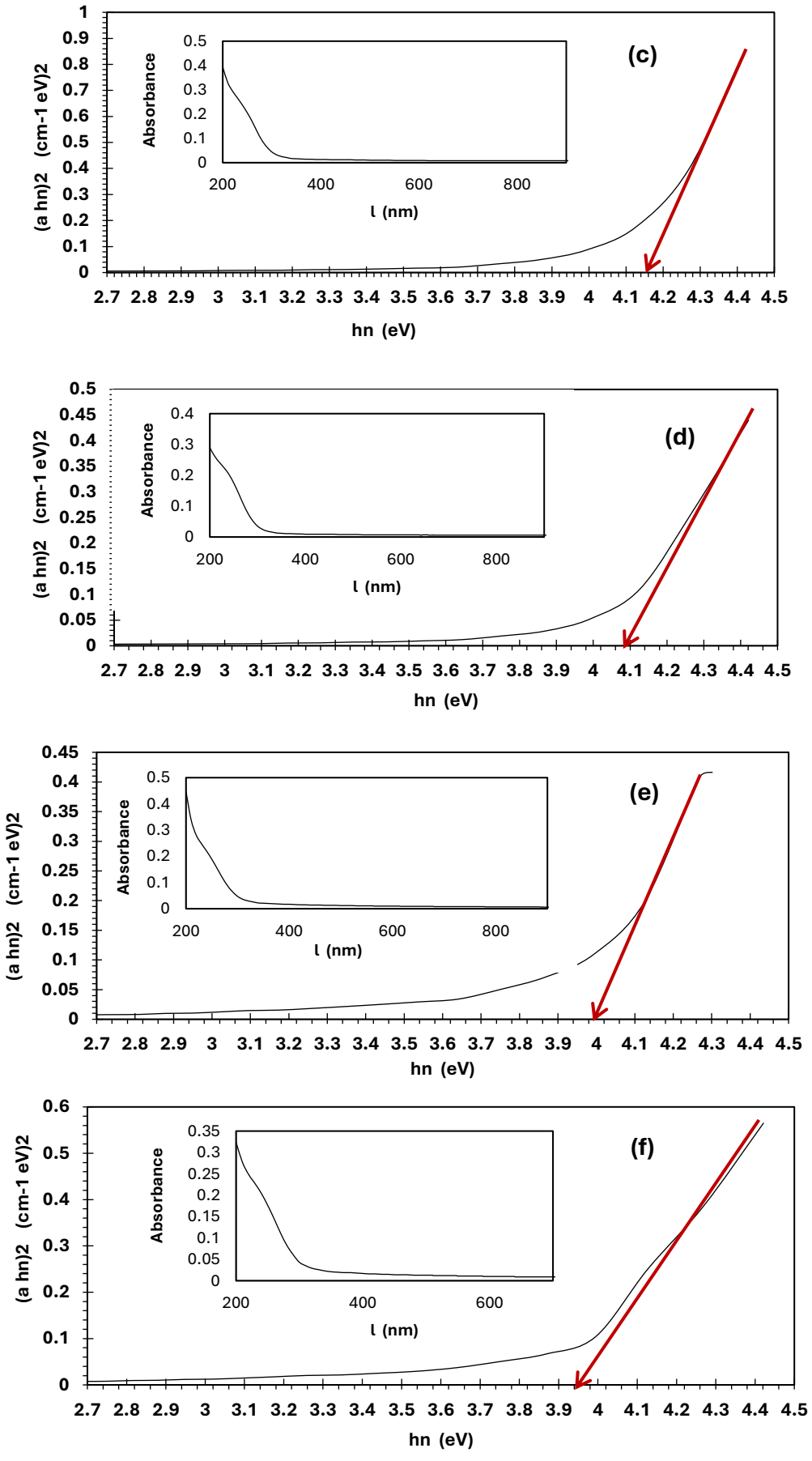

Figure 2. Absorption and bandgap energy plots of the prepared at various (a) 8.2 J/cm^2 , (b)10.18 J/cm^2, (c)12.09 J/cm^2, (d) 14 J/cm^2 , (e)15.91 J/cm^2 , and (f)17.82 J/cm^2.

Table 2 Energy bandgap obtained at different laser fluencies

Laser Fluence (J/cm^2)	Energy Bandgap (eV)
8.2	4.2
10.18	4.19
12.09	4.15
14	4.08
15.91	4
17.82	3.93

The spherical nanoparticles can be shown clearly in Figure (3) using Transmission Electron Microscopy images for samples prepared at different fluencies. Low concentrations of small, spherical-shaped particles are recognized at low laser fluence. Whereas, increasing the value of the laser fluence shows an increasing the particle size due to a high aggregation rate of high-concentration small fragments. Similar results are found in the literature referenced at [48-50].

Image J. software was used to perform TEM imaging histogram. Table (3) lists and illustrates the histogram curves of the average particle size. Its values were found to decrease with increasing laser fluence due to the large absorbed amount of energy. This phenomenon led to a temperature rise, after which the particles started [49].

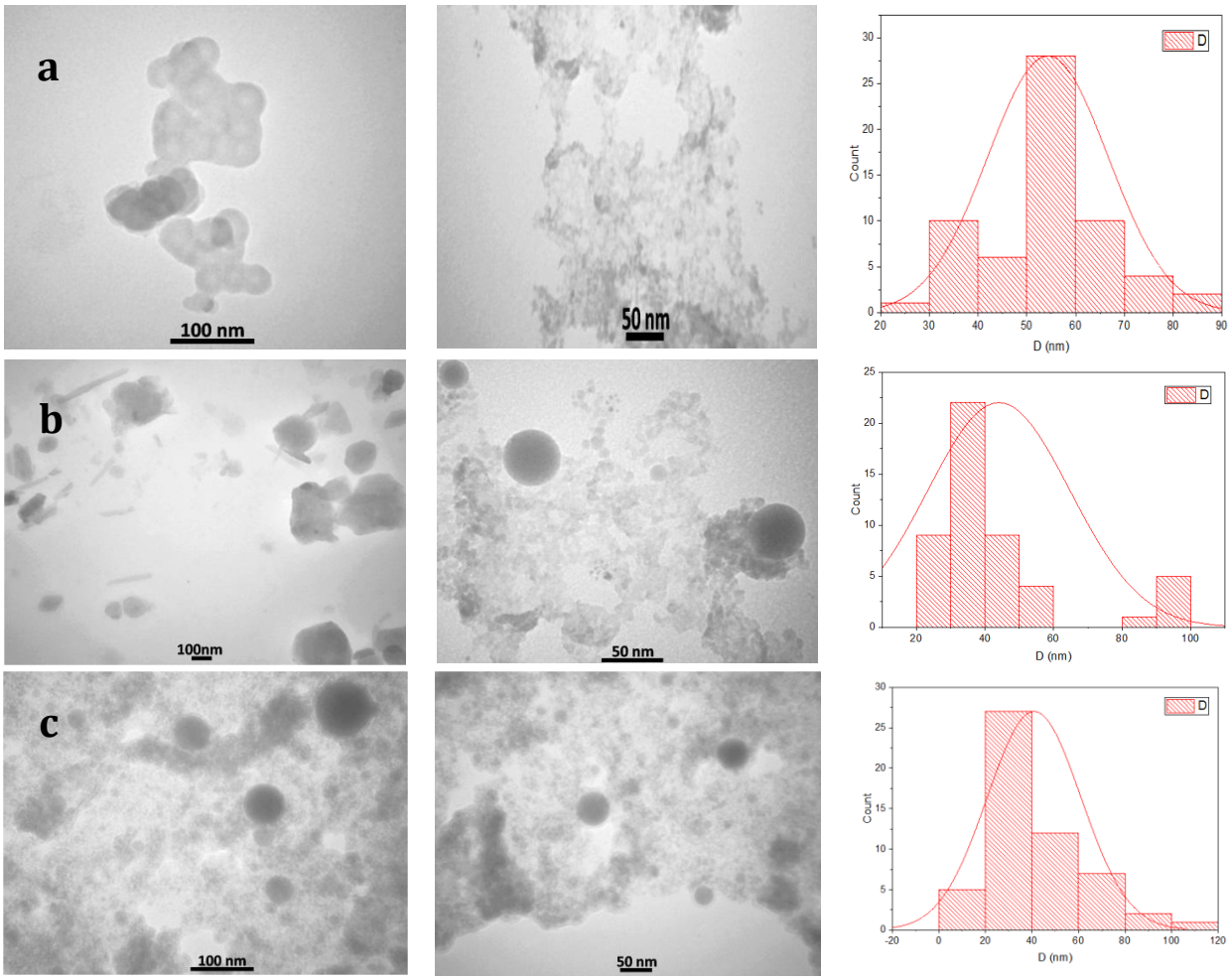

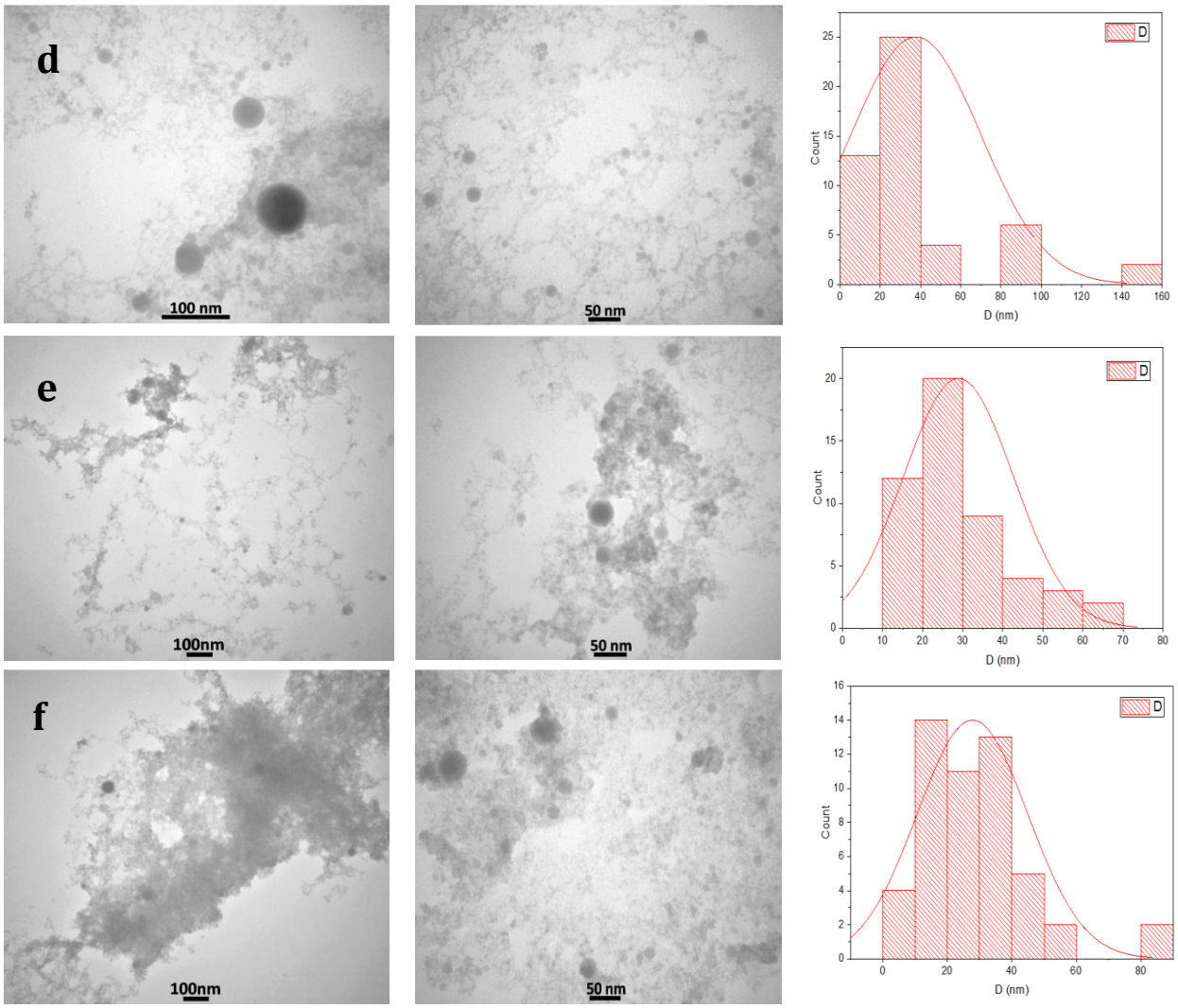

Figure 3. TEM images of the prepared samples at (a)8.2 J/cm^2 (b)10.18 J/cm^2 (c)12.09 J/cm^2 (d) 14 J/cm^2 (e)15.91 J/cm^2 (f)17.82 J/cm^2.

Table 3 Lists the average particle size in nanometers results are different laser fluences

Laser Fluence (J/cm^2)	Average particle size (nm)
8.2	55
10.18	45
12.09	42
14	40
15.91	30
17.82	28

According to previous results, the optimum results were achieved at a laser fluence value of 12.09 J/cm^2. Further measurements were conducted to understand the chemical behaviors of the prepared sample. Figure (4) shows the EDX image shows the optimal structural properties obtained by sample preparation at 12.09 J/cm^2 laser fluence. The appearance of Niobium, Oxygen, and both Carbon and Silicon are confirmed by the results obtained. The stoichiometry of Nb_2O_5 was approximately equal to 66.02%.

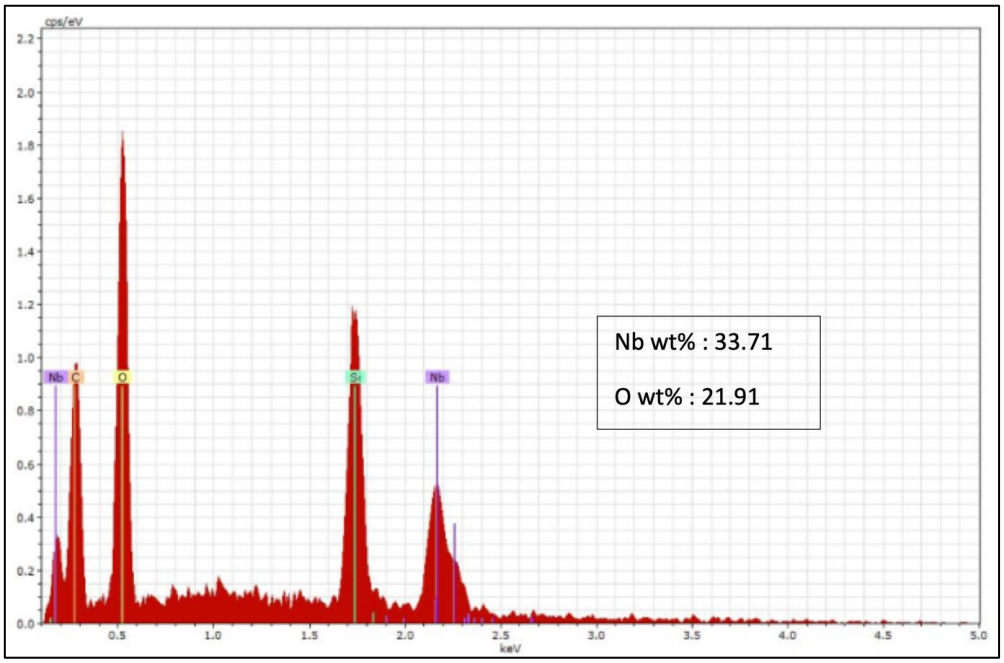

Figure 4. The EDX spectra of the prepared Nb_2O_5 at 12.09 J/cm^2.

Surface chemical bonds of Nb_2O_5 were investigated using FTIR spectroscopy. Figure (5) displays the FTIR transmission spectra of the Nb_2O_5 nanoparticles synthesized using 12.09 J/cm^2 laser fluence and 150 laser pulse. This fluence showed the best chemical bonds of Nb_2O_5. The FTIR spectra confirmed the existence of Nb_2O_5 and water.

Figure (5) shows the FTIR image of the prepared sample at 12.09 J/cm^2. The FTIR image depicts four transmission percentage peaks belonging to different wavenumbers. The first peak belongs to the stretching vibration mode of the "Nb-O-Nb" which occurred at 713.6 cm^{-1}. This peak commonly indicates the formation of the Nb_2O_5 and its T-Phase as stated in works references in [51-54]. The second peak is assigned to the bending vibration of the H_2O and the weak asymmetric band of the OH group which occurred at 1631.7 cm^{-1} as shown in other work [55, 56]. Finally, the peaks 2113.9 cm^{-1} and 3255.8 cm^{-1} are related to the pure niobium and the OH stretching vibration of Nb-OH, respectively [57-59].

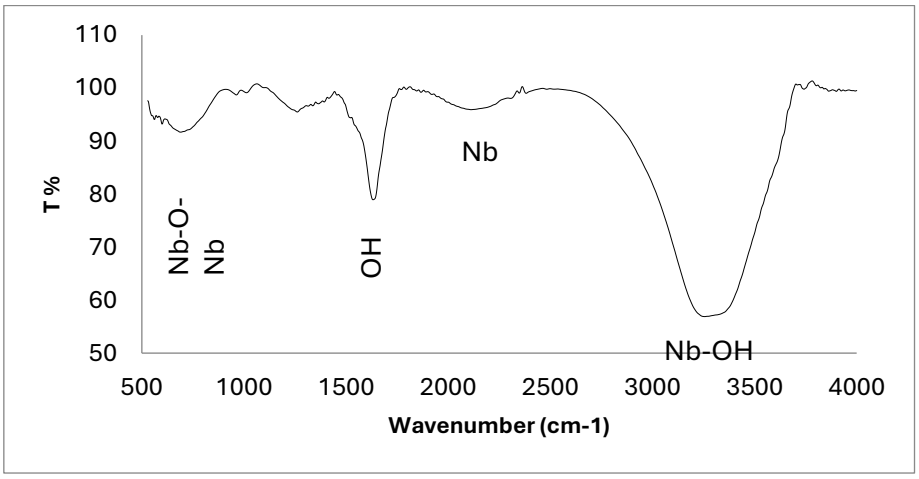

Figure 5. The FTIR of the prepared Nb_2O_5 at 12.09 J/cm^2.

According to the chemical bonds and the IR resonance peaks of the colloidal Nb_2O_5 are listed in Table (4). The locations of the observed peaks are completely agreed with works in literature listed in the same table.

Table 4 Represents the obtained chemical bonds and their position at 12.09 J/cm^2 laser fluence

Obtained bond value (cm^{-1})	Assignment	Vibration mode	Reference
713.6	Nb-O-Nb	Stretching	[51-54], [59, 60]
1631.7	O-H	Bending	[52, 55, and 61-63]
2113.98	Pure Nb		[57]
3255.84	Nb-OH	Stretching	[55, 62]

Raman spectroscopy is a very important non-destructive technique to characterize the chemical composition of Nb_2O_5. Figure (6) illustrates the Raman spectrum of Nb_2O_5 samples prepared using 12.09 J/cm^2 laser fluence and 150 pulse. This fluence provided the best Raman peaks, which represent the best chemical composition of Nb_2O_5. Raman spectrum of Nb_2O_5 Nanoparticles shows a peak 298.45 cm^{-1}, which indicates orthorhombic T-Nb_2O_5. The obtained results are concide with those obtained from FTIR and XRD tests. The small peak occurred at 649.15 cm^{-1} corresponds to the NbO_6 stretching modes of the typical polyhedra of the orthorhombic Nb_2O_5 crystalline structure [61-63]

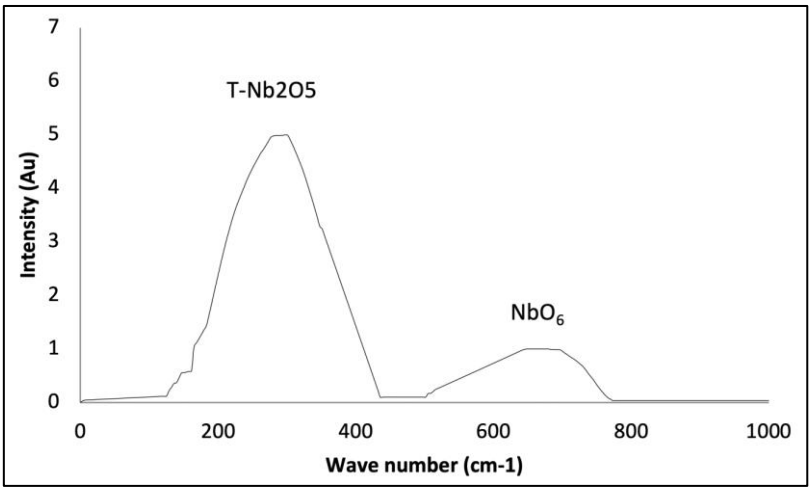

Figure 6. Raman spectra of the prepared Nb_2O_5 sample using 1064 nm Nd:YAG at 12.09 J/cm^2 with 150 pulse.

Details regarding the chemical bonds and their corresponding locations of the Raman peaks are listed in Table (5). The values of the observed peaks and their corresponding positions are highly agreed with FTIR and the results found in the literature which are mentioned in the table.

Table 5 Raman peaks for Nb_2O_5 nanoparticles corresponding chemical bonds

Peaks cm^{-1}	Peak Assigned to	Reference
298.45	T-Nb2O5 (orthorhombic structure)	[62]
649.15	Stretching modes of NbO6 polyhedral typical of orthorhombic structure	

4. CONCLUSIONS

In conclusion, spherical Nb_2O_5 nanoparticles were successfully synthesized using PLA. T-Nb_2O_5 structure was obtained, as confirmed using different measurements. Laser fluence influenced the properties of the prepared Nb_2O_5 nanostructured material in a liquid environment. The optimum laser flounce to prepare orthorhombic crystalline materials was 12.09 J/cm^2.

REFERENCE

[1] Nowak, I. and M.J.C.R. Ziolek, Niobium compounds: preparation, characterization, and application in heterogeneous catalysis. 1999. 99(12): p. 3603-3624.

[2] Evan T. Salim, Ahmed T. Hassan, Rana O Mahdi, Forat H. Alsultany, Physical Properties of HfO2 Nano Structures Deposited using PLD, IJNeaM, vol. 16, no. 3, pp. 495–510, Oct. 2023.

[3] Siddiki, M.K., S. Venkatesan, and Q.J.P.C.C.P. Qiao, Nb 2 O 5 as a new electron transport layer for double junction polymer solar cells. 2012. 14(14): p. 4682-4686.

[4] Yoshimura, K., et al., Niobium oxide electrochromic thin films prepared by reactive DC magnetron sputtering. 1995. 34(10A): p. L1293.
[5] Fang, X., et al., New ultraviolet photodetector based on individual Nb2O5 nanobelts. 2011. 21(20): p. 3907-3915.
[6] Jung, S.-C., N. Imaishi, and H.-C.J.J.J.O.A.P.P.L. Park, Reaction engineering modeling of low-pressure metalorganic chemical vapor deposition of Nb2O5 thin film. 1995. 34: p. L775-L775.
[7] Evan T. Salim, Rana O. Mahdi, Tamara E. Abdulrahman, Makram A. Fakhri, Jehan A. Siamon, Ahmad S. Azzahrani & Subash C.B. Gopinath, RE-crystallization of Nb2O5 nanocrystals: a study employing different laser wavelength, J Opt (2024). https://doi.org/10.1007/s12596-024-01942-7.
[8] Roberts, G., et al., Dielectric properties of barium titanium niobates. 1997. 12(2): p. 526-530.
[9] He, J., et al., Hydrothermal growth and optical properties of Nb 2 O 5 nanorod arrays. 2014. 2(38): p. 8185-8190.
[10] Roaa A. Abbas, Evan T. Salim & Rana O. Mahdi, Deposition time effect on copper oxide nano structures, an analysis study using chemical method, J Mater Sci: Mater Electron 35, 427 (2024). https://doi.org/10.1007/s10854-024-12143-0.
[11] Soares, M., et al., Effect of processing method on physical properties of Nb2O5. 2011. 31(4): p. 501-506.
[12] Falcomer, D., et al., Morphology and luminescence of nanocrystalline Nb2O5 doped with Eu3+. 2007. 2007.
[13] Zainab T. Hussain, Khawla S. Khashan, Rana O. Mahdi, Characterization of cadmium oxide nanoparticles prepared through Nd:YAG laser ablation process, Materials Today: ProceedingsVolume 42, Pages 2645 – 26482021. https://doi.org/10.1016/j.matpr.2020.12.594.
[14] Schäfer, H., R. Gruehn, and F.J.A.C.I.E.i.E. Schulte, The modifications of niobium pentoxide. 1966. 5(1): p. 40-52.
[15] Hassan M.A.M.; Al-Kadhemy M.F.H.; Salem E.T., Effect irradiation time of Gamma ray on MSISM (Au/SnO2/SiO2/Si/Al) devices using theoretical modeling, International Journal of Nanoelectronics and Materials, 8(2), 69-82 (2015).
[16] Jurn Y.N.; Malek F.; Mahmood S.A.; Liu W.-W.; Fakhri M.A.; Salih M.H., Modelling and simulation of rectangular bundle of single-walled carbon nanotubes for antenna applications Key Engineering Materials, 701, 57-66 (2016) 10.4028/www.scientific.net/KEM.701.57.
[17] Aegerter, M.A.J.S.e.m. and s. cells, Sol–gel niobium pentoxide: a promising material for electrochromic coatings, batteries, nanocrystalline solar cells and catalysis. 2001. 68(3-4): p. 401-422.
[18] Weibin, Z., et al., The investigation of NbO2 and Nb2O5 electronic structure by XPS, UPS and first principles methods. 2013. 45(8): p. 1206-1210.
[19] Azzam Y. Kudhur, Evan T. Salim, Ilker Kara, Makram A. Fakhri & Rana O. Mahdi, Structural optical and morphological properties of copper oxide nanoparticles ablated using pulsed laser ablation in liquid, J Opt 53, 1936–1945 (2024). https://doi.org/10.1007/s12596-023-01331-6.
[20] Salim, E.T., R.A. Ismail, and H.T.J.M.R.E. Halbos, Growth of Nb2O5 film using hydrothermal method: effect of Nb concentration on physical properties. 2019. 6(11): p. 116429.
[21] Coşkun, Ö.D. and S.J.A.s.s. Demirela, The optical and structural properties of amorphous Nb2O5 thin films prepared by RF magnetron sputtering. 2013. 277: p. 35-39.
[22] Rashed, R.S., Fakhri, M.A., Alwahib, A.A., Qaeed, M.A., Gopinath, S.C.B., Physical Investigations of GaN/Porous Silicon at Different Laser Wavelengths, International Journal of Nanoelectronics and Materials, 2024, 17(Special issue), pp. 77–86.
[23] Blanquart, T., et al., Evaluation and comparison of novel precursors for atomic layer deposition of Nb2O5 thin films. 2012. 24(6): p. 975-980.
[24] Joya, M.R., et al., Synthesis and characterization of nano-particles of niobium pentoxide with orthorhombic symmetry. 2017. 7(4): p. 142.
[25] Wang, X., et al., Caging Nb2O5 nanowires in PECVD-derived graphene capsules toward bendable sodium-ion hybrid supercapacitors. 2018. 30(26): p. 1800963.
[26] Dai, Q., et al., A novel nano-fibriform C-modified niobium pentoxide by using cellulose templates with highly visible-light photocatalytic performance. 2020. 46(9): p. 13210-13218.
[27] Fakhri M.A.; Numan N.H.; Mohammed Q.Q.; Abdulla M.S.; Hassan O.S.; Abduljabar S.A.; Ahmed A.A., Responsivity and response time of nano silver oxide on silicon heterojunction detector, International Journal of Nanoelectronics and Materials, 11(Special Issue BOND21), 109-114 (2018).
[28] Liu, J., D. Xue, and K.J.N.r.l. Li, Single-crystalline nanoporous Nb 2 O 5 nanotubes. 2011. 6(1): p. 1-8.
[29] Rana O. Mahdi, Aseel A. Hadi, Juhaina M. Taha, Khawla S. Khashan, Preparation of nickel oxide nanoparticles prepared by laser ablation in water, AIP Conf. Proc. 2213, 020309 (2020) https://doi.org/10.1063/5.0000116.
[30] Kumari, N., et al., Dependence of photoactivity of niobium pentoxide (Nb2O5) on crystalline phase and electrokinetic potential of the hydrocolloid. 2020. 208: p. 110408.
[31] Wang, X., et al., Orthorhombic niobium oxide nanowires for next generation hybrid supercapacitor device. 2015. 11: p. 765-772.
[32] Salim Z.T.; Hashim U.; Arshad M.K.M.; Fakhri M.A., Simulation, fabrication and validation of surface acoustic wave layered sensor based on ZnO/IDT/128° YX LiNBO3, International Journal of Applied Engineering Research, 11(15), 8785-8790 (2016).
[33] Kamlag, Y., et al., Laser CVD of cubic SiC nanocrystals. 2001. 184(1-4): p. 118-122.

[34] Khawla S. Khashan, Aseel A. Hadi, Rana O. Mahdi & Doaa S. Jubair, Aluminum-doped zinc oxide nanoparticles prepared via nanosecond Nd: YAG laser ablation in water: optoelectronic properties, Opt Quant Electron 56, 125 (2024). https://doi.org/10.1007/s11082-023-05630-x.

[35] Semaltianos, N., et al., CdTe nanoparticles synthesized by laser ablation. 2009. 95(3): p. 191.

[36] Abdul Muhsien M.; Salem E.T.; Agool I.R., Preparation and characterization of (Au/n-Sn O2 /Si O2 /Si/Al) MIS device for optoelectronic application, International Journal of Optics, 2013, 756402 (2013) 10.1155/2013/756402.

[37] Evan T. Salim, Rana O. Mahdi, Doaa Mahmoud, Subash C. B. Gopinath & Forat H. Alsultany, An Analysis Study Employing Laser Ablation in Gold Colloidal at Different Numbers of Laser Pulses, Plasmonics (2025). https://doi.org/10.1007/s11468-025-02998-2.

[38] Bushroa, A.R., et al., Approximation of crystallite size and microstrain via XRD line broadening analysis in TiSiN thin films. 2012. 86(8): p. 1107-1112.

[39] Hattab F.; Fakhry M., Optical and structure properties for nano titanium oxide thin film prepared by PLD, 2012 1st National Conference for Engineering Sciences, FNCES 2012, 6740474 (2012) 10.1109/NCES.2012.6740474.

[40] Khawla S. Khashan, Jehan A. Saimon, Aseel A. Hadi and Rana O. Mahdi, Influence of laser energy on the optoelectronic properties of NiO/Si heterojunction, J. Phys.: Conf. Ser. 1795 (2021) 012026. DOI 10.1088/1742-6596/1795/1/012026.

[41] Intartaglia, R., et al., Luminescent silicon nanoparticles prepared by ultra short pulsed laser ablation in liquid for imaging applications. 2012. 2(5): p. 510-518.

[42] Kabashin, A.V. and M.J.J.o.A.P. Meunier, Synthesis of colloidal nanoparticles during femtosecond laser ablation of gold in water. 2003. 94(12): p. 7941-7943.

[43] Chen, K.-N., et al., Investigation of antireflection Nb2O5 thin films by the sputtering method under different deposition parameters. 2016. 7(9): p. 151.

[44] Nunes, B.N., et al., Recent advances in niobium-based materials for photocatalytic solar fuel production. 2020. 10(1): p. 126.

[45] Ismail R.A.; Salim E.T.; Halbos H.T., Preparation of Nb2O5 nanoflakes by hydrothermal route for photodetection applications: The role of deposition time, Optik, 245, 167778 (2021) 10.1016/j.ijleo.2021.167778.

[46] Fakhri, Makram A, Alwahib, Ali Abdulkhaleq, Ibrahim, Raed Khalid, Salim, Evan T.,Abbas, Abeer R., Alsultany, Forat H., Gopinath, Subash C. B.,Qaeed, Motahher A.,Effect of different laser wavelengths on the optical properties of GaN/PSi and Al_2O_3/PSi thin films using the pulse laser deposition method, Journal of Optics (India), 2025, 475402, 10.1007/s12596-024-02393-w.

[47] Azzam Y. kudhur, Evan T. Salim, Ilker Kara, Rana O. Mahdi & Raed K. Ibrahim, The effect of laser energy on Cu2O nanoparticles formation by liquid-phase pulsed laser ablation, J Opt 53, 1309–1321 (2024). https://doi.org/10.1007/s12596-023-01319-2.

[48] Nichols, W.T., T. Sasaki, and N.J.J.o.a.p. Koshizaki, Laser ablation of a platinum target in water. III. Laser-induced reactions. 2006. 100(11): p. 114911.

[49] Imam, H., et al., Effect of experimental parameters on the fabrication of gold nanoparticles via laser ablation. 2012.

[50] Jehan A. Saimon, Suzan N. Madhat, Khawla S. Khashan, Azhar I. Hassan, Rana O. Mahdi, Rafah A. Nasif, Synthesis of $Cd_xZn_{1-x}O$ nanostructure films using pulsed laser deposition technique, AIP Conf. Proc. 2045, 020003 (2018) https://doi.org/10.1063/1.5080816.

[51] Huang, Y.-T., et al., Solution-based synthesis of ultrasmall Nb2O5 nanoparticles for functional thin films in dye-sensitized and perovskite solar cells. 2017. 236: p. 131-139.

[52] Vicentini, R., et al., Core-niobium pentoxide carbon-shell nanoparticles decorating multiwalled carbon nanotubes as electrode for electrochemical capacitors. 2019. 434: p. 226737.

[53] Alsultany F.H.; Alhasan S.F.H.; Salim E.T., Seed Layer-Assisted Chemical Bath Deposition of Cu2O Nanoparticles on ITO-Coated Glass Substrates with Tunable Morphology, Crystallinity, and Optical Properties, Journal of Inorganic and Organometallic Polymers and Materials, 31(9), 3749-3759 (2021) 10.1007/s10904-021-02016-y.

[54] Orel, B., et al., In situ UV-Vis and ex situ IR spectroelectrochemical investigations of amorphous and crystalline electrochromic Nb 2 O 5 films in charged/discharged states. 1998. 2(4): p. 221-236.

[55] Ristić, M., S. Popović, and S.J.M.L. Musić, Sol–gel synthesis and characterization of Nb2O5 powders. 2004. 58(21): p. 2658-2663.

[56] Fatema H. Rajab, Rana M. Taha, Aseel A. Hadi, Khawla S. Khashan & Rana O. Mahdi , Laser induced hydrothermal growth of ZnO rods for UV detector application, Opt Quant Electron 55, 208 (2023). https://doi.org/10.1007/s11082-022-04473-2.

[57] Cardoso, F.P., et al., Effect of tungsten doping on catalytic properties of niobium oxide. 2012. 23: p. 702-709.

[58] Salim, E.T., Saimon, J.A., Abood, M.K., ...Alsultany, F.H., A Preliminary Study on Structural and Optical Properties of Heat Treated Nb2O5 Nanostructure, International Journal of Nanoelectronics and Materials, 16(1), pp. 21-32 (2023).

[59] Athar, T., et al., One-pot synthesis and characterization of Nb2O5 nanopowder. 2012. 12(10): p. 7922-7926.

[60] Tamara E Abdulrahman, Evan T Salim, Rana O Mahdi and MHA Wahid, Nb2O5 nano and microspheres fabricated by laser ablation, Advances in Natural Sciences: Nanoscience and Nanotechnology, Volume 13, Number4, 045006 (2022), DOI 10.1088/2043-6262/ac99cf.

[61] Pawlicka, A., M. Atik, and M.A.J.T.S.F. Aegerter, Synthesis of multicolor Nb2O5 coatings for electrochromic devices. 1997. 301(1-2): p. 236-241.
[62] Raba-Paéz, A.M., et al., Niobium pentoxide samples with addition of manganese at different concentrations and calcination temperatures applied in the photocatalytic degradation of rhodamine B. 2020. 10(12): p. 4257.
[63] Salim E.T.; Halboos H.T., Synthesis and physical properties of Ag doped niobium pentoxide thin films for Ag-Nb2O5/Si heterojunction device, Materials Research Express, 6(6), 66401 (2019) 10.1088/2053-1591/ab07d3.